Available online at www.sciencedirect.com
SCIENCE DIRECT
Cancer Letters 245 (2007) 218–231
CANCER Letters
www.elsevier.com/locate/canlet

Apoptosis of human melanoma cells induced by the novel compounds propolin A and propolin B from Taiwenese propolis

Chia-Nan Chen [a], Chia-Li Wu [b], Jen-Kun Lin [a,*]

[a] *Graduate Institute of Biochemistry and Molecular Biology, College of Medicine, National Taiwan University, Section 1, Jen-Ai Road, Taipei 100, Taiwan, ROC*
[b] *Department of Chemistry, Tamkang University, Tamsui 251, Taiwan, ROC*

Received 12 September 2005; received in revised form 8 December 2005; accepted 16 January 2006

Abstract

We recently demonstrated that two new prenylflavanones, propolin A and propolin B, isolated and characterized from Taiwanese propolis, induced cytotoxicity effect in human melanoma A2058 cells and shows a strong capability to scavenge free radicals. In this study, propolin A effectively induced a cytotoxic effect on five different cancer cell lines. Similar results were obtained for propolin B. DNA flow cytometric analysis and DNA fragmentation ladder indicated that propolin A and propolin B actively induced apoptosis in A2058 cells. To address the mechanism of the apoptosis effect of propolin A and propolin B, we evaluated the apoptosis-related proteins in A2058 cells. The levels of procaspase-8, Bid, procaspase-3, DFF45, and PARP were decreased in dose- and time course-dependent manners. Furthermore, also found propolin A and propolin B was capable of releasing cytochrome *c* from mitochondria to cytosol. The findings suggest that propolin A and propolin B may activate a mitochondria-mediated apoptosis pathway. On the other hand, our data show that propolin B inhibitied xanthine oxidase activity more efficiently than propolin A or CAPE. However, CAPE suppressed ROS-induced DNA strand breakage more efficiently than propolin A or propolin B. All these results indicated that propolin A and propolin B may trigger apoptosis of A2058 cells through mitochondria-dependent pathways and also shown that propolin A and propolin B were strong antioxidants.

Keywords: Propolin A; Propolin B; Taiwanese propolis; Apoptosis; Xanthine oxidase; Human melanoma cells

1. Introduction

A natural honeybee product, propolis, is a resinous material gathered by honey bees from the buds and bark of certain trees and plants, and used inside their hives [1]. It is a kind of crude medicine that has long been used as a folk remedy chiefly in Europe [2]. Propolis contains various chemical components and exhibits a broad spectrum of biological activities including antitumor [3], antioxidant [4], antibacterial [5], antiviral [6], antifungal [7], and anti-inflammatory activities [7].

Many natural products used in cancer chemotherapy, including taxol [8], adriamycin [9], VP16 [10], and camptothecin [10], have apoptosis-inducing activity. We previously identified two novel prenylflavanones from Taiwanese propolis, flavonoid compounds with hydrated geranyl side chains, namely, propolin A and propolin B (Fig. 1) [11]. Flavonoids are found naturally in fruits and vegetables and have been indicated in chemoprevention or anticancer activity [12,13]. The anticancer activities of flavonoids are due to induced apoptosis [14]. Many flavonoids have also been shown to induce apoptosis in cancer cells include quercetin

* Corresponding author. Tel.: +886 2 2356 2213; fax: +886 2 2391 8944.
E-mail address: jklin@ha.mc.ntu.edu.tw (J.-K. Lin).

0304-3835/$ - see front matter © 2006 Elsevier Ireland Ltd. All rights reserved.
doi:10.1016/j.canlet.2006.01.016

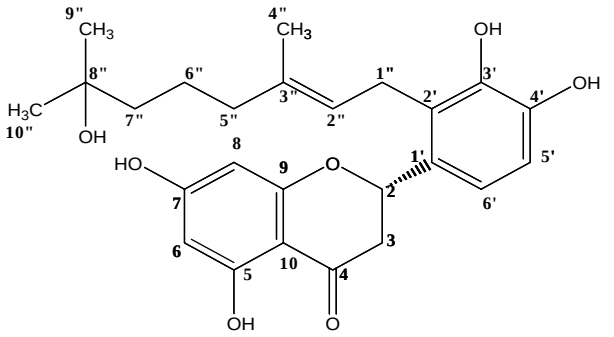

Propolin A

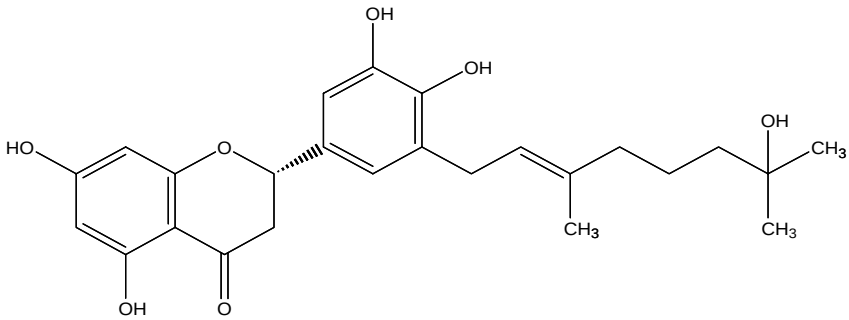

Propolin B

Fig. 1. Structures of propolin A and propolin B.

[15], bicalein [16], genistein [17], tangeritin [18] and sophoranone [19]. Propolin A and propolin B have hydrated geranyl side chains that differ from these flavonoids, but chemical structures similar to sophoranone that it has isoprenyl side chains.

Apoptosis, the physiological mode of cell death, is related to the regulation of development and homeostasis. Its morphological characteristics include plasma membrane blebbing, cell shrinkage, nuclear condensation, chromosomal DNA fragmentation, and formation of apoptotic bodies [20]. Many recent reports have indicated that many anticancer drugs or cancer chemopreventive agents act through the induction of apoptosis to prevent tumor promotion and progression. The process of apoptosis consists of different phases, including initiation, execution and degradation [21], and is activated by two major pathways. One is receptor-induced apoptosis that includes of the TNF-R1, Fas (CD95), and TRAIL-receptors [22,23]. In the so-called 'extrinsic' cell death pathway, a cytoplasmic death domain forms and trimerization of the receptor (TNF-R1, Fas, and TRAIL) and recruits TRADD and FADD. The other major route leading to apoptosis is the 'intrinsic' cell death pathway, activated by proapoptotic factors from the mitochondria, including cytochrome *c* and Apaf-1 [24,25].

We have demonstrated that propolin A and propolin B are cytotoxic to human melanoma A2058 cells, rat C6 glioma cells, and human leukemia cells (HL-60). In the present study, both propolin A and propolin B were found effectively induced cytotoxic effects of several cancer cell lines occur in a dose-dependent manner. Furthermore, we demonstrate that apoptosis induced by propolin A and propolin B in A2058 cells may through caspases-dependent pathways, and also that propolin A and propolin B can significantly inhibit xanthine oxidase activity, suggesting that they are strong antioxidants.

2. Materials and methods

2.1. Cell culture and cytotoxicity assay

Human melanoma cells (A2058), human breast cancer cells (MCF-7), human neuroblastoma cells (IMR-32), and rat glioma cells (C6) were cultured in Dulbecoo's modified Eagle's medium (DMEM, Gibco) containing 10% fetal bovine serum (Gibco) 1% penicillin–streptomycin. Cells were maintained at 37 °C in a humidified atmosphere at

95% air and 5% CO_2. Human leukemia cells (HL-60) grown were maintained at 37 °C in a humidified atmosphere at 95% air and 5% CO_2 in RPMI 1640 media supplemented with 10% fetal bovine serum and 1% penicillin–streptomycin. All cells (1×10^5)/well were cultured in twelve-well plates and in the presence of various concentrations 0, 5, 10, and 15 μg/mL (0, 11.4, 22.8, and 34.2 μM, respectively) of propolin A (MW = 442 Da) and propolin B (MW = 442 Da) for 24 h. Treated cells were counted and cell viability was determined by a trypan blue exclusion assay.

2.2. Isolation of propolin A and propolin B

Taiwanese propolis glue (245 g, mixture from a collection of hives located in area of Bagwa Shan, Taiwan) was homogenized by stirring at 4 °C and washed thrice with 0.7 L of deionized water. The residue was extracted three times with 95% ethanol. The filtered ethanol extract was evaporated to dryness under reduced pressure to furnish a brown powder, which was kept at −20 °C until further purification. The brown powder from the ethanol extract was dissolved in methanol and applied to a Sephadex LH-20 column (Amersham Pharmacia Biotech AB, Uppsala, Sweden) using 95% ethanol as eluting solvent. All eluates, including fractions from the follow-up chromatographies, were assayed on human melanoma A2058 cells proliferation, and the active fractions were again chromatographed on Sephadex LH-20 column using 95% ethanol to elute. The active fractions were then subjected to silica gel column chromatography (Kiesel gel 60, E. Merck, Darmstadt 1, Germany) using a solvent system of *n*-hexane–EtOAc. Purification of the most active fraction (*n*-hexane:EtOAc = 30:70) was carried out on a reversed-phase preparative HPLC. Fractions of retention times at 16.5 min, and 22.0 min containing propolins A, and B, respectively, were collected. The conditions were: column-Luna Phenomenex (C18, 250×10 mm, USA), solvent system: methanol:water (7:3); flow rate: 3 mL/min; detection: UV 280 nm. Propolin A and propolin B were obtained as a slightly yellow powder from methanol:water (7:3).

2.3. Analysis of DNA fragmentation

A2058 cells in a 60-mm dish were treated with various concentrations of propolin A and propolin B (11.4–34.2 μM) for 24 h, trypsinized, and collected with ice-cold PBS. After centrifugation 2000×*g* for 10 min at 4 °C, cells were washed with PBS and recentrifuged at 13200×*g* for 10 min at 4 °C. Cell pellets were resuspended in 0.1 mL of isolation buffer (10 mM EDTA, 50 mM Tris–HCl, pH 8.0, 0.5% SDS, 1 mg/mL proteinase K) and incubated 12 h at 50 °C and treated with RNase A (0.5 μg/mL) for another 4 h at 37 °C. The lysate was centrifuged at 13,200×*g* for 10 min at 4 °C to separate the soluble fragmented DNA from the intact chromatin pellet. Fragmented DNA was extracted with phenol:chloroform:isoamylalcohol (25:24:1), precipitated with ethanol, and analyzed by 1.8% agarose gel electrophoresis. Approximately 20 μg DNA was loaded in each well visualized under UV light, and photographed.

2.4. Morphological analysis of apoptotic cells

A2058 cells on 60-mm culture dishes (5×10^5 /dish) were treated with propolin A at concentrations of 11.4, 22.8, and 34.2 μM for 24 h. After treatments, cells were fixed with 4% formaldehyde for 30 min, washed with PBS, and then stained with 50 μg/mL propidium iodide (PI) in the presence of 25 μg/mL RNase A. The morphology of nuclear chromatin was defined by the fluorescence of DNA-binding dye, PI, under a fluorescence microscope (Zeiss, Jena, Germany).

2.5. Analysis of the cell cycle

A2058 cells (1×10^6) were cultured in 60-mm dishes and incubated for 24 h. Cells were then treated with 5.7, 11.4, 22.8, and 34.2 μM of propolin A and propolin B for 24 h cells were trypsinized and collected with ice-cold PBS. The cells were resuspended in 200 μL PBS, and fixed in 800 μL of iced 100% ethanol at −20 °C. After being left to stand overnight, the cell pellets were collected by centrifugation, resuspended in 1 mL of hypotonic buffer (0.5% Triton X-100 in PBS and 0.5 μg/mL RNase A), and incubated at 37 °C for 30 min Then 1 mL of propidium iodide solution (50 μg/mL) was added, and the mixture was allowed to stand at 4 °C for 30 min fluorescence emitted from the propidium iodide–DNA complex was quantitated after exicitation of the fluorescent dye by FACScan cytometry (Becton Dickinson, San Jose, CA).

2.6. Supercoiled DNA-relaxation assay

The inhibitory effect of propolin A, propolin B, and CAPE on the strand breakage of supercoiled DNA caused by the Fenton reaction was evaluated. 200 ng of pUC-19 plasmid DNA was incubated at 37 °C for 30 min in TE buffer (10 mM Tris/1 mM EDTA, pH 8.0) containing 100 mM H_2O_2 and 50 μM ferrous sulfate in the presence or absence of 10–105 μM CAPE and 7–68 μM propolin A and propolin B in a final volume of 20 μL. The conversion of the covalently closed circular double-stranded supercoiled DNA to a relaxed open circle form was used to evaluate DNA strand breakage induced by the Fenton reaction. Such breaks occurred rapidly, with most of the supercoiled pUC-19 NDA converted to open circular form after 30 min incubation at 37 °C. The reaction was terminated by the addition of 4 μL of electrophoresis loading buffer (0.25% bromophenol blue and 30% glycerol). After electrophoreses on an agarose gel, the percentage of relaxed DNA was calculated by a Gel-doc 2000 (Bio-Rad).

2.7. Xanthine oxidase activity assay

The enzyme activity was measured spectrophotometrically by continuously measuring uric acid formation at 295 nm with xanthine as substrate [26]. The xanthine oxidase assay consisted of a 500 μL reaction mixture containing 7.5 mM phosphate buffer, 20 mM 3-(cyclohexylamino)-1-propanesulfonic acid (CAPS), 38 μM EDTA (pH 7.0), 3 U/L xanthine oxidase, and 50 μM xanthine as substrate. The assay was started by addition of the enzyme to the reaction mixture with or without propolin A, propolin B and CAPE. The assay mixture was incubated for 3 min at 37 °C and absorbency readings were taken. The substrate concentration was held below 60 μM to avoid substrate inhibition. All data obtained for enzyme inhibition assays and plotting were recorded using Microsoft Excel, Office 2000.

2.8. Western blotting assay

A2058 cells on 100-mm culture dishes (1.5×10^6 /dish) were treated with propolin A and propolin B at 5.7, 11.4, 17.0, 22.8, and 34.2 μM for 24 h. After treatment, cells were collected and resuspended in 100 μL Gold lysis buffer (50 mM Tris–HCl, pH 7.4; 1 mM NaF; 150 mM NaCl; 1 mM EGTA; 1 mM phenylmethylsulfonyl floride; 1% NP-40; and 10 μg/mL leupeptin). Equal amounts of proteins (20 μg) were mixed with 5× sample buffer and resolved by 12% SDS-PAGE for β-actin, PARP, Bid, caspase-3, Fas ligand, Fas, Bcl-2 and cytochrome *c* detection. Proteins were electrotransferred to an immobilon membrane (PVDF; Millipore Corp., Bedford, MA), and equivalent protein loading was verified by staining the membrane with reversible dye amido black (Sigma Chemical Co.). This was followed by overnight blocking with a solution composed of 20 mM Tris–HCl (pH 7.4), 125 mM NaCl, 0.2% Tween 20, 4% nonfat dry milk, and 0.1% sodium azide. Expression of β-actin, PARP, Bid, caspase-3, Fas, Fas ligand, Bcl-2 and cytochrome *c* was monitored by immunoblotting using a specific antibody (1:500 of rabbit polyclonal antibodies to human PARP, Santa Cruze Biotechnology, Inc., Santa Cruz, CA), anti-caspase-3 antibody and anti-caspase-8 antibody (Pharmingen, Becton Dickinson Co., San Diego, CA), anti-Bid antibody (Santa Cruze Biotechnology, Inc., Santa Cruz, CA), anti-actin antibody (Cashmere Biotech, USA), and cytochrome *c* antibody (Research Diagnostic Inc., Flanders, NJ). Anti-Fas and Fas L (Santa Cruze Biotechnology, Inc., Santa Cruz, CA), anti-Bcl-2 and DFF45 antibody (Pharmingen, Becton Dickinson Co., San Diego, CA). These proteins were detected by chemiluminescence (ECL, Amersham).

2.9. Cytochrome c release

Mitochondrial and cytosolic fractions were prepared by resuspending cells in ice-cold buffer A (250 mM sucrose, 20 mM HEPES, 10 mM KCl, 1.5 mM $MgCl_2$, 1 mM EDTA, 1 mM EGTA, 1 mM DTT, 17 μg/mL PMSF, 8 μg/mL aprotinin and 2 μg/mL leupeptin pH 7.4). Cells were passed through a needle 10 times. Unlysed cells and nuclei were pelleted by centrifugation for 10 min at $750\times g$. The supernatant was then centrifuged at $100{,}000\times g$ for 15 min. This pellet was resuspended in buffer A and represents the mitochondrial fraction. The supernatant was again centrifuged at $100{,}000\times g$ for 1 h. The supernatant from this final centrifugation step represents the cytosolic fraction.

2.10. Activity of caspase

Cells were collected and washed with PBS and suspended in 25 mM HEPES (pH 7.5), 5 mM $MgCl_2$, 5 mM EDTA, 5 mM dithiothione, 2 mM phenylmethylsulfonylfluoride, 10 μg/mL pepstatin A and 10 μg/mL leupeptin after treatment. Cell lysates were clarified by centrifugation at $13{,}200\times g$ for 20 min at 4 °C. Caspase activity in the supernatant was determined by a fluorogenic assay (Promega's CasACE™ assay system, Madison, WI). Briefly, 75 μg of total protein, as determined by bicinchoninic acid assay (Promega), was incubated with 50 μM substrate acetyl-Asp-Glu-Val-Asp-7-amino-4-methyl coumarin (Ac-DEVD-AMC) at 30 °C for 1 h. The release of AMC was measured by excitation at 360 nm and emission at 460 nm using a fluorescence spectrophotometer (Hitachi F-4500).

2.11. Statistical analysis

In the cell blockage of propolin A-induced cell death by caspase inhibitors experiments, A2058 (3×10^5 per well) cells were cultured in six-well plates and incubated with the indicated concentrations of propolin A in the absence or presence of caspase inhibitors (1, 3, 6, 8, and total) for 24 h. Viability assay as measured by using trypan blue exclusion assay. Each value represents the mean ± S.E. of three independent measurements. Viability assay data were entered into the sigma plot software to perform the Student's pair-*t* test. P values <0.05 were considered significant.

3. Results

3.1. Purification and identification of propolin A and propolin B

Propolin A and propolin B were isolated through repeated chromatographies of the 95% ethanol extract of the propolis glue under the guidance of A2058 cells proliferation. Final purification of the active fraction was achieved by HPLC on a reversed-phase column. The total content of the active components, propolin A and propolin B were roughly 3.0 and 1.0% of the Taiwaneses propolis glue. Purification of propolin A and propolin B as described in Section 2.

3.2. Inhibition of cell growth by propolin A and propolin B

The cytotoxicity effect of propolin A and propolin B (Fig. 1) were first evaluated in the A2058 cells, C6, MCF-7, IMR-32, and HL-60. As shown in Fig. 2, treatment with propolin A and propolin B concentrations of 5.7–34.2 μM caused a dose-dependant decrease of cell viability. The IC_{50} values of propolin A on the A2058, C6, MCF-7, IMR-32 and HL-60 were 14.5, 8.0, 14.0, 11.4, and 17.5 μM, respectively, as shown in Fig. 2a. Similar results were obtained for propolin B, as shown in Fig. 2b. Among the cell lines tested, propolin A and propolin B in cell viability assay showed no significant differences. Treatment of the A2058 cells with 22.8–34.2 μM propolin A and propolin B for 24 h induced cell morphological change as shown in Fig. 2c. Morphological features, such as condensation of chromatin of the nucleus and cell shrinkage, were seen in propolin A- and propolin B-treated cells. It appears that the cells morphologic changes may be via induced apoptosis as described below.

3.3. Induction of apoptosis by propolin A and propolin B

We next questioned whether propolin A and propolin B induced apoptosis in A2058 cells. After treatment of A2058 cells with various concentrations of propolin A and propolin B for 24 h, the genomic DNA from cells was subjected to agarose gel electrophoresis. The DNA fragmentation ladder significantly increased as shown in Fig. 3a. The induction of apoptosis was further, confirmed in fluorescence photomicrographs of human melanoma cells stained with PI after treatment with 22.8 μM propolin A and propolin B for 24 h. The morphological features of apoptosis, such as condensation of chromatin and fragmentation of the nucleus into discrete masses scattered throughout the cytosol, were seen in propolin A- and propolin B-treated cells (Fig. 3b). To investigate the induction of a sub-G1 cell population, the DNA content of A2058 cells treated with propolin A and propolin B at various concentrations was analyzed by flow cytometry as shown in Fig. 3c. The percentages of apoptotic A2058 cells observed after 0, 5.7, 11.4, 22.8 and 34.2 μM of propolin A [left column in Fig. 3c] and propolin B [right column in Fig. 3c] for 24 h were as follows: 9.4, 12.2, 11.7, 22.6, and 26.1% [propolin A] vs. 9.5, 8.9, 11.2, 23.7, and 25.1% [propolin B]. A sub-G1 (sub-2N) DNA peak, which has been suggested to be the apoptotic DNA, was detected. However, we next questioned whether cell damage might be attributable to the cell cycle program or might have become arrested at any cell cycle phases by propolin A- and propolin B-induced apoptosis in A2058 cells. These results show that propolin A and propolin B efficiently induced apoptosis in the A2058 cells, and there is a marked loss of cells from the G2/M phase of the cell cycle. These results show that propolin A and propolin B had cytotoxic effects on five cancer cell lines, and the cytotoxic effects may be through apoptosis induction

3.4. Propolin A induced apoptosis via activated caspase- and mitochondrial-dependent pathway

We first evaluate whether caspase-dependent signal pathways were involved in the apoptotic cell death induced by propolin A in A2058 cells. Treatment of A2058 cells with 11.4–34.2 μM of propolin A for 24 h resulted in dramatic decreases in procaspase-8 and Bid protein levels (Fig. 4a). Next, we further evaluate whether cytochrome *c* release from mitochrondria to cytosol during the induction of apoptosis by propolin A. Our data indicated cytochrome *c* was markedly released from mitochondria to cytosol as shown in Fig. 4b. We next questioned whether propolin A can activation of caspase-9, caspase-3 and cleavage of PARP, and DFF45 finally form DNA fragmentation. Our data indicated these protein expression were markedly decreased by treated with propolin A at concentrations of 22.8–34.2 μM (Fig. 4c). However, we also findings that Fas and Fas L protein expression were markedly increased by treated with propolin A at concentrations of 22.8–34.2 μM (Fig. 4c). Furthermore, we used 20 μM of caspase inhibitors (1, 3, 6, 8, and total) to block the cell death induced by propolin A at a concentration of 22.8 μM (Fig. 4d). The results indicated that activation of caspase-8, and caspase-3 by propolin

Fig. 2. Effect of propolin A and propolin B on the viability of human melanoma A2058 cells, C6 glioma cells, MCF-7 human breast cancer cells, IMR-32 human neuroblastoma cells and HL-60 human leukemia cells. (a) The cells were treated with various concentrations (5.7–34.2 μM) of propolin A and (b) propolin B for 24 h and subsequent cell viability was measured by a trypan blue exclusion assay. The data are presented in terms of proportional viability (%) by comparing the propolin A and propolin B treated group with the untreated cells, the viability, of which was assumed to be 100%. Results represent the mean ± SE of three independent experiments. (c) Phase-contrast micrographs of A2058 cells treated with various concentrations of propolin A and propolin B (22.8–34.2 μM). Results are from one experiment representative of three similar experiments. Magnification ×400.

(a)

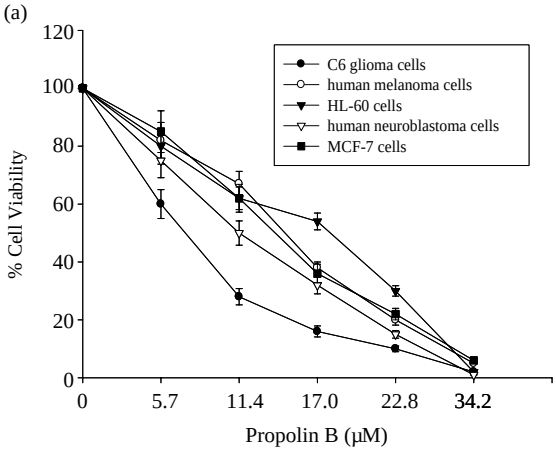
C6 glioma cells
human melanoma cells
HL-60 cells
human neuroblastoma cells
MCF-7 cells
% Cell Viability
120
100
80
60
40
20
0
0
5.7
11.4
17.0
22.8
34.2
Propolin B (μM)

(b)

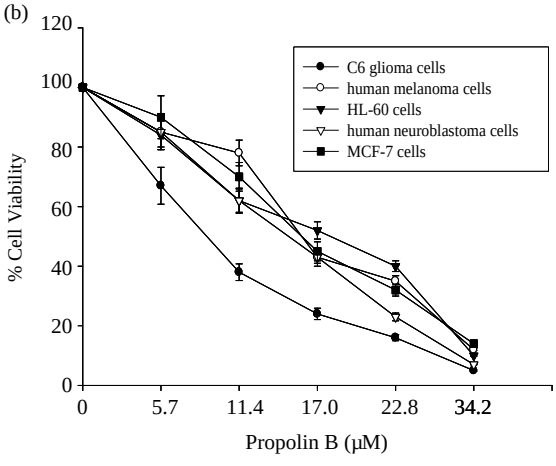
C6 glioma cells
human melanoma cells
HL-60 cells
human neuroblastoma cells
MCF-7 cells
% Cell Viability
120
100
80
60
40
20
0
0
5.7
11.4
17.0
22.8
34.2
Propolin B (μM)

(c)

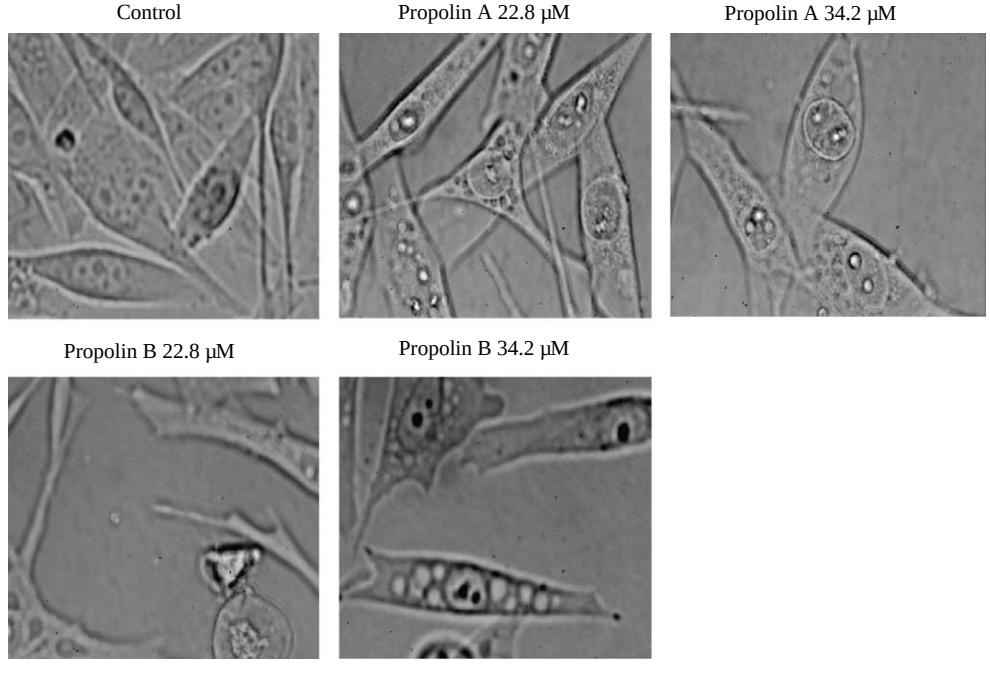
Control
Propolin A 22.8 μM
Propolin A 34.2 μM
Propolin B 22.8 μM
Propolin B 34.2 μM

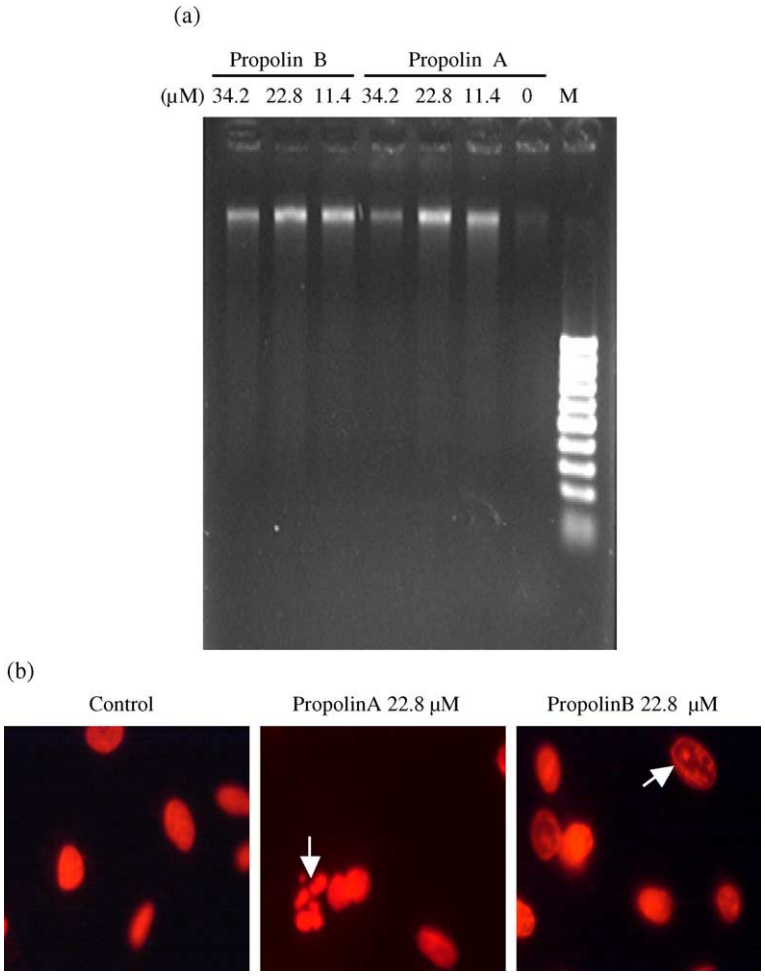

Fig. 3. Propolin A- and propolin B-induced DNA fragmentation in A2058 cells. (a) DNA fragmentation by propolin A and propolin B in A2058 cells. A2058 cells were treated with various concentrations of propolin A and propolin B (11.4–34.2 μM) for 24 h. Genomic DNA was isolated and analyzed by 1.8% agarose gel electrophoresis. (b) Effect of propolin A and propolin B on the morphology of nuclear chromatin. The untreated and propolin A or propolin B (22.8 μM) treated cells for 24 h were fixed and stained as described in Section 2. Morphological changes of nuclear chromatin were then viewed under a fluorescence microscope. Control cells showed round and homogeneous nuclei; whereas apoptotic cells (arrows) showing condensed and fragmented nuclei were observed in the propolin A and propolin B-treated cells. Results are from one experiment representative of three similar experiments. Magnification ×400. (c) Effect of propolin A and propolin B on the cellular DNA content. The cells were treated with various concentrations (5.7–34.2 μM) of propolin A and propolin B for 24 h and stained with PI as described in Section 2. Following flow cytometric analysis, cellular DNA profile was further analyzed by the CellQuest software. Data represent the percentage of cell counts displaying a hypoploid DNA population. Results are from one experiment that is representative of three similar experiments.

A may be due behind the induction of apoptosis in A2058 cells.

3.5. Propolin B induced apoptosis via activated caspase- and mitochondrial-dependent pathway

We further, evaluated whether propolin B had activity similar to propolin A. Treatment of A2058 cells with 11.4–34.2 μM propolin B for 24 h the proteins expression of procaspase-3, PARP, DFF45, and Bcl-2 were markedly decreased as shown in Fig. 4e. We further, investigated whether propolin B induced apoptosis through a mitochondrial-dependent pathway. Treatment of A2058 cells with 11.4, 22.8, and 34.2 μM propolin B for 24 h resulted in dramartic decreases in procaspase-8 and Bid protein expression and induced cytochrome *c* releasing from mitochondria to cytosol (Fig. 4f). These results together indicated that the propolin A and propolin B caused caspases activation and up-regulation of the Fas L and through the mitochondrial-dependent pathway to induce apoptosis in A2058 cells.

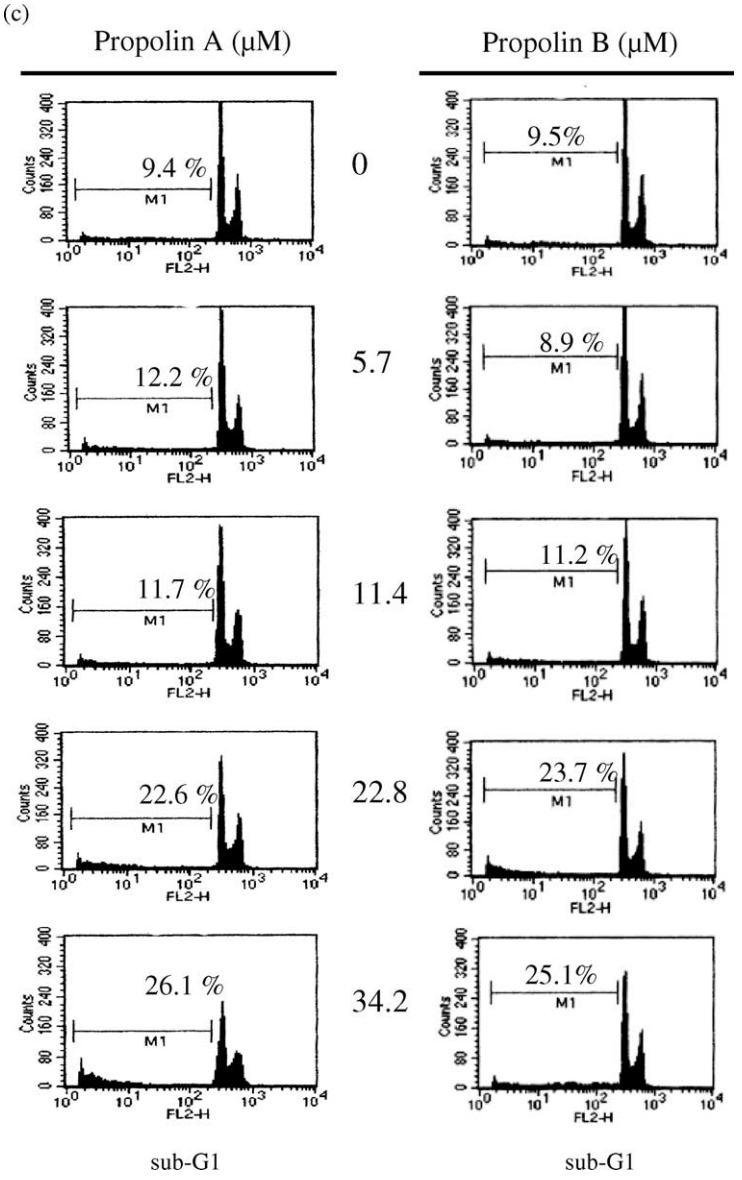

Fig. 3 (*continued*)

3.6. Caspase-3 activation of A2058 cells by propolin A and propolin B

To further investigated the mechanisms of propolins A- and B-induced apoptosis, we think of the possible involvement of caspases. Activation of caspase-3 plays an important role in the induction of apoptosis by various stimuli [27]. Upon treatment of A2058 cells with 34.2 μM propolin A, the activity of a caspase-3-like enzyme increased significantly within 12 h after the start of treatment (Fig. 5). An even faster activation of a caspase-3-like enzyme occurred within 6 h after the start of treatment with 34.2 μM propolin B (Fig. 5). The results further obtained in these experiments suggested that caspase-3 involved in propolins A- and B-induced apoptosis of A2058 cells.

3.7. Inhibition of xanthine oxidase by propolin A, propolin B, and CAPE

Xanthine oxidase (XO) is a major source of reactive oxygen species (ROS). Normal loads of ROS are removed by the enzyme superoxide dismutase (SOD), catalase, and glutathione peroxidase. Excessive

amounts of ROS increase oxidative stress in the body, accelerating membrane damage, DNA base oxidation, DNA strand breaks, and chromosome aberrations, most of which are involved in the cacinogenesis process [28]. The effects of three polyphenols on XO activity were tested, and the dose-response curves and IC_{50} values for these three compounds are shown in Fig. 6a. The IC_{50} values of propolin A, propolin B, and CAPE [29] (caffeic acid phenethyl ester was an active compound isolated from propolis) were 32, 23, and 44 μM, respectively. In the system, the IC_{50} value for the well-known XO inhibitor allopurinol is 0.7 μM (data not shown). The results suggest that the chemical structures of propolin A and propolin B are closely related to hypoxanthine, xanthine, and uric acid structure may act as substrate analogs for XO.

3.8. Propolin A suppressed ROS induced DNA strand breakage

Hydroxyl radical (·OH) generated by the fenton reaction is known to cause oxidatively induced DNA strand breaks to yield open circular DNA (relaxed circular DNA). Hydroxyl radical scavengers can protect DNA from strand breaks induced by hydroxyl radical. The hydroxyl radical scavenger ability of propolin A,

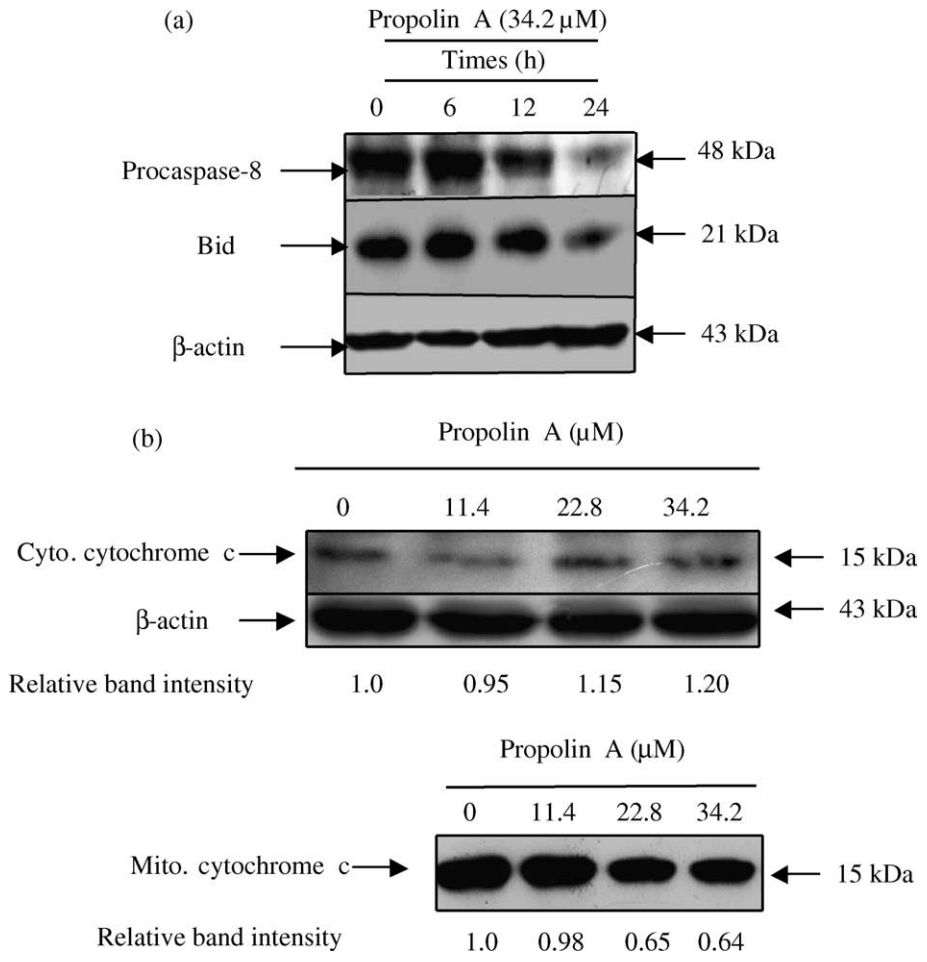

Fig. 4. Induction of apoptosis via caspase- and mitochondrial-dependent pathway. A2058 cells were incubated with 11.4, 22.8, and 34.2 μM concentrations of propolin A for 24 h. Cell lysates were prepared, and subjected to SDS-PAGE. (a) Procaspase-8, and Bid were determined by immunoblotting using specific antibodies. (b) Cytochrome *c* was released from mitochondria into the cytosol. (c) Fas, Fas L, Bid, Bcl-2, DFF45, procaspase-3 and PARP were determined by immunoblotting using specific antibodies. Proteins were visualized using the ECL system. (d) Blockage of propolin A-induced cell death by caspase inhibitors. A2058 cells were incubated with 22.8 μM propolin A in the absence or presence of caspase inhibitors (1, 3, 6, 8, and total) for 24 h. Viable cells were determined using by a trypan blue exclusion assay. Each data represents the mean ± S.E. of three independent experiments. (e) A2058 cells were incubated with 11.4, 22.8, and 34.2 μM concentrations of propolin B for 24 h. Cell lysates were prepared, subjected to SDS-PAGE, and determined by immunoblotting using specific antibodies. (f) Procaspase-8, Bid, and *cytochrome* were determined by immunoblotting using specific antibodies.

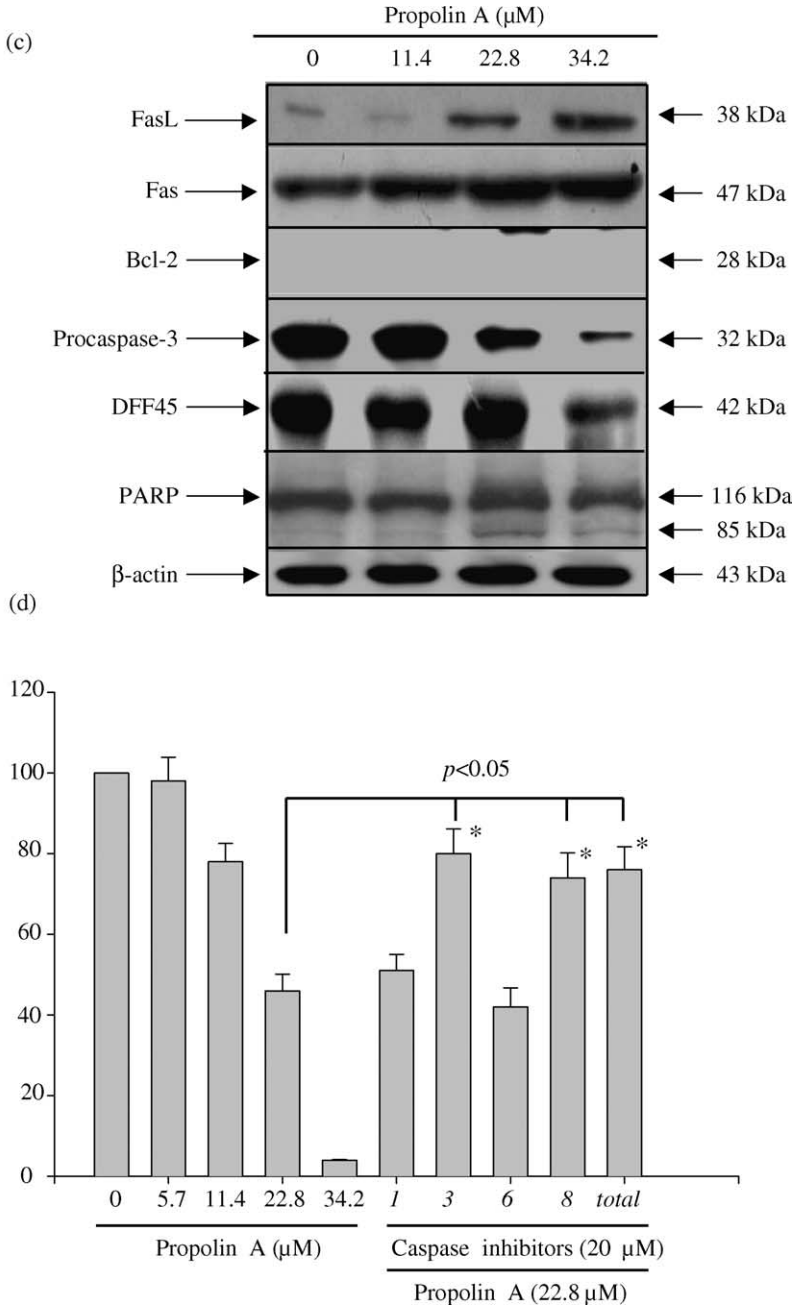

Fig. 4 (*continued*)

propolin B, and CAPE were evaluated. Supercoiled DNA migrates faster than relaxed circular DNA on agarose gel electrophoresis. DNA strand breakage was induced in vitro in the presence of H_2O_2 and Fe^{2+} (lane 2, Fig. 6b), while DNA in the absence of H_2O_2 and Fe^{2+} did not show significant strand breakage (lane 1, Fig. 6b). Treatment of DNA with propolin A, propolin B, and CAPE significantly reduced the concentration of relaxed circular DNA in a dose-dependent manner (Fig. 6b). The results indicated that propolin A and propolin B are potential antioxidant agents.

4. Discussion

Propolis is a folk medicine used for the treatment of various ailments, and has been demonstrated to have

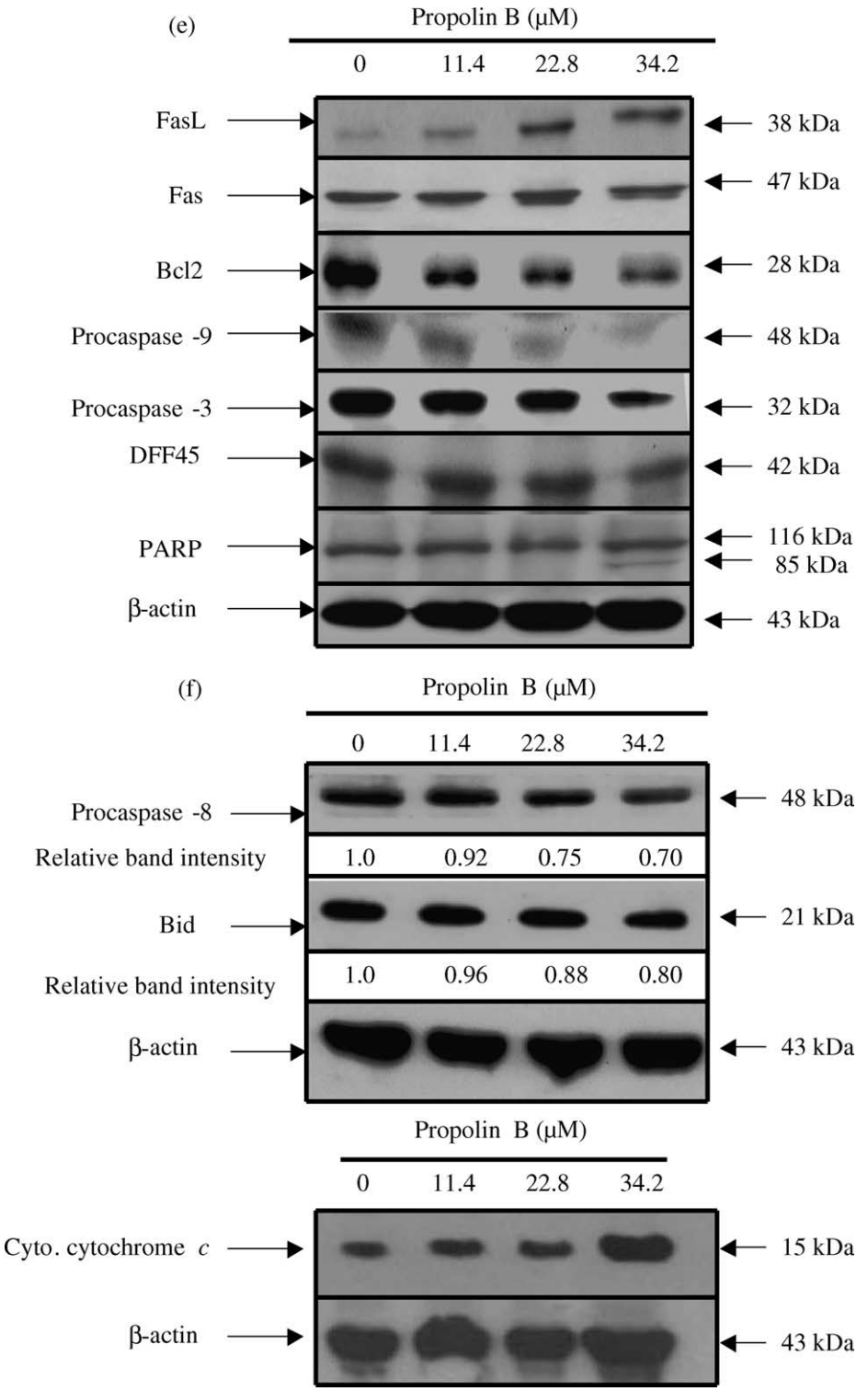

Fig. 4 (*continued*)

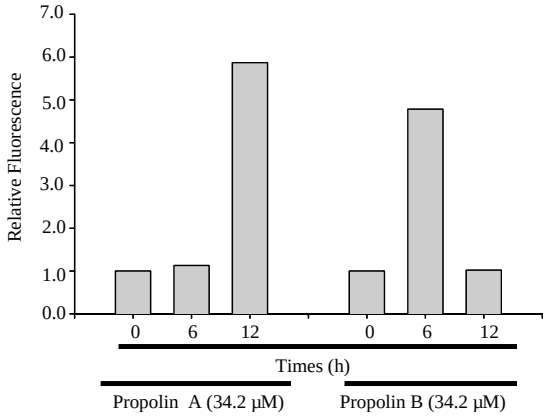

Fig. 5. Analysis of the caspase-3-like activity induced by propolin A and propolin B. A2058 cells were treated with 34.2 μM propolin A and propolin B for the indicated times and caspase-3-like activity in cell extracts was measured with a specific fluorogenic substrate. Results are representative of the results of three separate experiments.

a broad spectrum of activities [2]. To investigate the chemical constituents of Taiwanese propolis with anti-cancer activity, we first isolated two new cytotoxic compounds, the structures of propolin A and propolin B has been characterized by NMR and HRMS spectra, which are depicted in Fig. 1. We have been shown that propolin A and propolin B, caused dose-dependent changes in five cancer cell lines at low dosages as shown in Fig. 2a and b. Chemical structure studies indicated that propolin A and propolin B were flavonoid compounds with hydrated geranyl side chains. A closely related compound, nymphaeol B, from *Hernandia nymphaefolia* has also been reported [30]. However, no biological activities of this compound have ever been reported. Another closely related compound sophoranone, has been reported to induce apoptosis in human leukemia U937 cells [19]. Hyperforin was isolated from St John's wort (*Hypericum perforatum*), and inhibition of tumor cell growth by it has been reported [31]. Many reports have

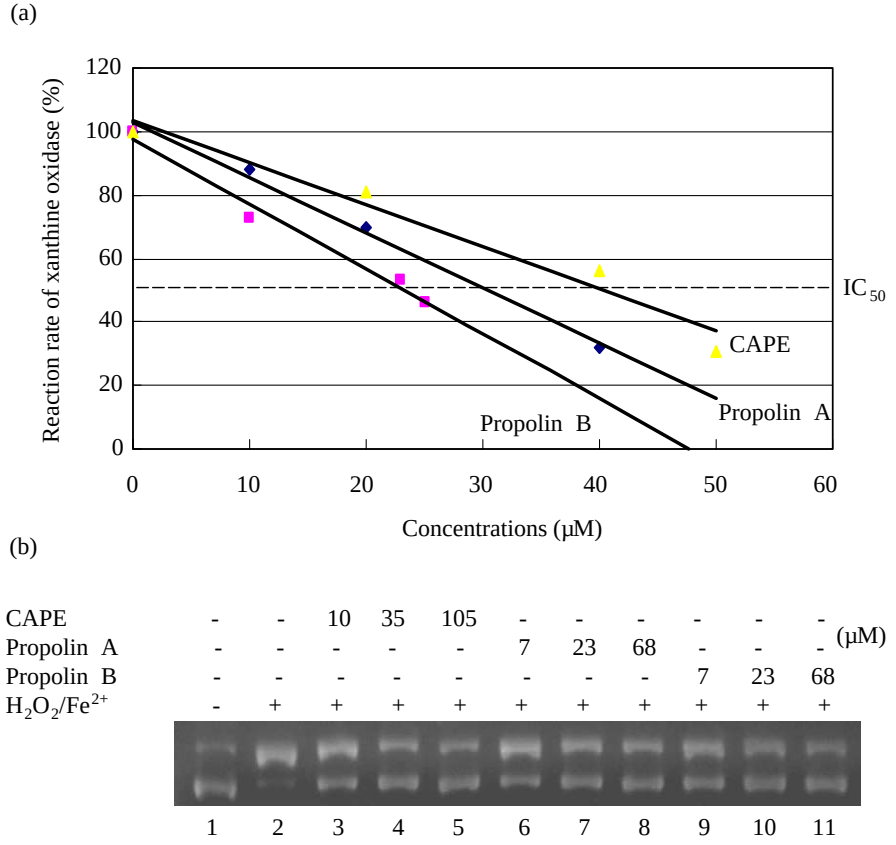

Fig. 6. Antioxidant activity of propolin A and propolin B. (a) Inhibition of xanthine oxidase by propolin A, propolin B, and CAPE. The formation of uric acid was determined spectrophotometrically at 295 nm as described in Section 2. (b) Propolin A, propolin B, and CAPE suppressed ROS induced DNA strand breakage. Plasmid DNA was incubated at 37 °C for 30 min with 100 mM H_2O_2 and 50 μM ferrous sulfate in the presence or absence of propolin A, propolin B, and CAPE.

indicated that geranylgeranylacetone [32] or vitamin K_2 with 4 isoprene units [33], significantly inhibit cell growth and induce the differentiation of leukemia cells.

In this study, we have demonstrated that propolin A and propolin B potently inhibits the proliferation of A2058 cells through inducing a cytotoxic effect and triggering apoptosis. Apoptosis can be evaluated by three techniques: DNA laddering, fluorescence microscope, and flow cytometry. When A2058 cells were grown in the presence of propolin A and propolin B and cells were isolated and analyzed electrophoretically for nuclear DNA degradation as shown in Fig. 3a, the results indicated that propolin A and propolin B markedly promoted DNA fragmentation at a concentration of 22.8 μM. A2058 cells were grown in the presence of various concentrations of propolin A and propolin B (11.4–34.2 μM) for 24 h and cells were analyzed by flow cytometry. Results indicated that propolin A and propolin B efficiently induced apoptosis in A2058 cells, and there is a clear loss of cells from the G2/M phase of the cell cycle as shown in Fig. 3c. We further, investigated the molecular mechanism of the propolin A and propolin B induced apoptosis pathway. Our data indicated that propolin A can increases of Fas and Fas L protein levels expression, and activation of procaspas-8, Bid, procaspase-3, PARP, and DFF45, finally producing DNA fragmentation (Fig. 4). On whether propolin A induced apoptosis through the mitochondrial-dependent pathway, our data indicated that it can increase cytochrome *c* release from mitocondrial to cytoplasm (Fig. 4b).

When cells were pretreated with caspase inhibitor, including caspase-1, -3, -6, -8, and total for 1 h, then treated with 22.8 μM propolin A for 24 h, to evaluate cell viability. Our data demonstrated that only caspase-3 and -8 significantly prevented cell death, but caspase-1 and -6 did not. All these results indicated that propolin A induced apoptosis via activated caspase-dependent pathway.

Propolin B-induced apoptosis may perhaps occur through the same or another pathway in A2058 cells. Western blotting showed that propolin B markedly inhibited of Bcl-2 expression and also the activation of caspase-8, Bid, caspase-3, DFF45, and PARP. The caspase-3-like activity assay indicated that propolin B was active within 6 h after the start of treatment while propolin A was active within 12 h. Taken together, we think that propolin A and B may act through partial different pathways to induce cancer cell apoptosis.

Previous studies have indicated that propolin A and propolin B exert antioxidant properties. We further study that propolin A and propolin B antioxidant assay in XO activity and ROS induced DNA strand breakage. Our data demonstrated that propolin A, propolin B, and CAPE might inhibit XO activity IC_{50} values at concentrations of 22, 23, 44 μM, respectively (Fig. 6a). Propolin A and propolin B chemical structure have flavanols group closely hypoxanthine, xanthine, and uric acid structure may be as substrate for XO, but CAPE chemical structure was not closely for xanthine may be not as substrate. On the other hand, propolin A and propolin B can scavenge of hydroxyl radical and protect DNA from strand breaks induced by hydroxyl radical (Fig. 6b), but CAPE has more strength to scavenge free radicals than propolin A or propolin B. In the present study, we demonstrated that both compounds have strong antioxidant activity and induce apoptosis in different cancer cell lines. However, how do these two antioxidant agents trigger apoptosis in A2058 cells? We think that propolin A and B (polyphenolic compounds) can be oxidized and can exert pro-oxidant effects in some culture media conditions. Many studies have demonstrated that rapid generation of H_2O_2 can occur on addition of EGC, EGCg, catechin, and quercetin to commonly used culture media [34,35]. These results could explain that propolin A and B may be via rapid generation of H_2O_2 to induce cells cytotoxicity or apoptosis.

Recently, many reports have suggested that the caspase family plays an important role in apoptosis. The caspases are unique in their requirement for an Asp residue at the cleavage site in their substrates. Recently, 14 known members of the caspases family of proteases, caspase-3 have been suggested to be a key role of the apoptotic machinery. Fas/Fas ligand (Fas L) death pathway is an important mediator of apoptosis. Deregulation of Fas pathway is reported to be involved in the immune escape of breast cancer and the resistance to anti-cancer drug [36]. In this study, we results indicated that the Fas/Fas ligand pathway of cell death signalling is involved in propolin A-induced apoptosis in A2058 cells.

In summary, we think that propolin A- and propolin B-induced apoptosis may be a result of modulated Fas and Fas L expression, further activation of caspase-8, and Bid, and induced cytochrome *c* release from mitochondria to the cytosol, and activation of caspase-3 to cleave PARP and cause DNA fragmentation, finally resulting in the execution of apoptosis in A2058 cells.

Acknowledgements

We thank Chun-Mao Lin and Chiung-Ho Liao for providing excellent technical supports.

References

[1] G.A. Burdock, Review of the biological properties and toxicity of bee propolis, Food Chem. Toxicol. 36 (1998) 347–363.
[2] E.L. Ghisalberti, Propolis: a review, Bee World 60 (1979) 59–84.
[3] C. Gunduz, C. Biray, B. Kosova, B. Yilmaz, Z. Eroglu, F. Sahin, et al., Evaluation of Manisa propolis effect on leukemia cell line by telomerase activity, Leuk. Res. 29 (2005) 1343–1346.
[4] M.R. Ahn, S. Kumazawa, T. Hamasaka, K.S. Bang, T. Nakayama, Antioxidant activity and constituents of propolis collected in various areas of Korea, J. Agric. Food Chem. 52 (2004) 7286–7292.
[5] L.C. Lu, Y.W. Chen, C.C. Chou, Antibacterial activity of propolis against *Staphylococcus aureus*, Int. J. Food Microbiol. 102 (2005) 213–220.
[6] M. Heluihel, V. Isanu, Anti-herpes simplex virus effect of an aqueous extract of propolis, Isr. Med. Assoc. J. 4 (2002) 923–927.
[7] J.W. Dobrowolski, S.B. Vohora, K. Sharma, S.A. Shah, S.A. Naqvi, P.C. Dandiya, Antibacterial, antifungal, antiamoebic, anti-inflammatory and antipyretic studies on propolis bee products, J. Ethnopharmacol. 35 (1991) 77–82.
[8] K. Bhalla, A.M. Ibrado, E. Tourkina, C. Tang, M.E. Mahoney, Y. Huang, Taxol induces internucleosomal DNA fragmentation associated with programmed cell death in human myeloid leukemia cells, Leukemia 7 (1993) 563–568.
[9] C. Friesen, I. Herr, P.H. Krammer, K.M. Debatin, Involvement of the CD95 (Apo-1/Fas) receptor/ligand system in drug-induced apoptosis in leukemia cells, Nat. Med. 2 (1996) 574–577.
[10] S.H. Kaufmann, Induction of endonucleolytic DNA cleavage in human acute myelogenous leukemia cells by etoposide, camptothecin, and other cytotoxic anticancer drugs: a cautionary note, Cancer Res. 49 (1989) 5870–5878.
[11] C.N. Chen, C.L. Wu, H.S. Shy, J.K. Lin, Cytotoxic prenylflavanones from Taiwanese propolis, J. Nat. Prod. 66 (2003) 503–506.
[12] B. Stavric, Role of chemopreventers in human diet, Clin. Biochem. 27 (1994) 319–332.
[13] Y. Matsukawa, N. Marui, T. Sakai, Y. Satomi, M. Yoshida, K. Matsumoto, et al., Genistein arrests cell cycle progression at G2-M, Cancer Res. 53 (1993) 1328–1331.
[14] K. Yanagihara, A. Ito, T. Toge, M. Numoto, Antiproliferative effects of isoflavones on human cancer cell lines established from the gastrointestinal tract, Cancer Res. 53 (1993) 5815–5821.
[15] Y.Q. Wei, X. Zhao, Y. Kariya, K. Fukata, K. Teshigawara, A. Uchida, Induction of apoptosis by quercetin: involvement of heat shock protein, Cancer Res. 54 (1994) 4952–4957.
[16] Y. Matsuzaki, N. Kurokawa, S. Terai, Y. Matsumura, N. Kobayashi, K. Okita, Cell death induced by bicalein in human hepatocellular carcinoma cell lines, Jpn. J. Cancer Res. 87 (1996) 170–177.
[17] W. Gorczyca, J. Gong, B. Ardelt, F. Traganos, Z. Darzynklewiez, The cell cycle-related differences in susceptibility of HL-60 cells to apoptosis induced by various antitumor agents, Cancer Res. 53 (1993) 3186–3192.
[18] T. Hirano, K. Abe, M. Gotoh, K. Oka, Citrus flavone tangeretin inhibits leukemia HL-60 cell growth partially through induction of apoptosis with less cytotoxicity on normal lymphocytes, Br. J. Cancer 72 (1995) 1380–1388.
[19] K. Sachiko, T. Noriko, K. Tetsuya, X. Man, C. Judong, M. Yutaka, et al., Sophoranone, extracted from a traditional Chinese medicine *shan dou gen*, induces apoptosis in human leukemia U937 cells via formation of reactive oxygen species and opening of mitochondrial permeability transition pores, Int. J. Cancer 99 (2002) 879–890.
[20] A.H. Wyllie, Apoptosis: an overview, Br. Med. Bull. 53 (1997) 451–465.
[21] G. Kroemer, The proto-oncogene Bcl-2 and its role in regulating apoptosis, Nat. Med. 3 (1997) 614–620.
[22] A. Ashkenazi, V.M. Dixit, Death receptors: signaling and modulation, Science 281 (1998) 305–308.
[23] M.J. Martinez-Lorenzo, S. Alava, K.J. Gamen, A. Kim, A. Chuntharapai, J. Pineiro, et al., Involvement of APO2 ligand/TRAIL in activation-induced death of Jukat and human peripheral blood T cells, Eur. J. Immunol. 28 (1998) 2714–2725.
[24] N.A. Thornberry, Y. Lazebnik, Caspases: enemies within, Science 281 (1998) 1312–1316.
[25] J.C. Reed, Cytochrome *c*: can't live with it-can't live without it, Cell 91 (1997) 559–562.
[26] W.S. Chang, Y.H. Chang, F.J. Lu, H.C. Chiang, Inhibitory effects of phenolics on xanthine oxidase, Anticancer Res. 14 (1994) 501–506.
[27] A.J. Darmon, D.W. Nicholson, R.C. Bleackley, Activation of the apoptotic protease CPP32 by cytotoxic T-cell-derived granzyme B, Nature 377 (1995) 446–448.
[28] P.A. Cerutti, Prooxidant states and tumor promotion, Science 227 (1985) 375–380.
[29] D. Grunberger, R. Banerjee, K. Eisinger, E.M. Oltz, L. Efros, M. Caldwell, et al., Preferential cytotoxicity on tumor cells by caffeic acid phenethyl ester isolated from propolis, Experientia 44 (1988) 230–232.
[30] Y. Kenichi, S. Kenichi, M. Hiroyuki, F. Hiroshi, New prenylflavanones from hernandia nymphaefolia (Presl) kubitzki, Heterocycles 14 (1980) 397–401.
[31] M.S. Christoph, K. Vladimir, S.H. Birgit, K. Astrid, C.T. Judit, G. Christian, et al., Inhibition of tumor cell growth by hyperforin, a novel anticancer durg from St John's wort that acts by induction of apoptosis, Oncogene 21 (2002) 1242–1250.
[32] I. Sakai, T. Tanaka, S. Osawa, S. Hashimoto, K. Nakaya, Geranylgeranylacetone used as an antiulcer agent is a potent inducer of differentiation of various human myeloid leukemia cell lines, Biochem. Biophys. Res. Commun. 191 (1993) 873–879.
[33] I. Sakai, M. Yoda, T. Hida, S. Osawa, S. Nakajo, K. Nakaya, Novel role of vitamin K2 a potent inducer of differentiation of various human myeloid leukemia cell lines, Biochem. Biophys. Res. Commun. 205 (1994) 1305–1310.
[34] H.L. Lee, V.C. Marie, H. Barry, Artifacts in cell culture: rapid generation of hydrogen peroxide on addition of (−)-epigallocatechin, (−)-epigallocatechin gallate, (+) catechin, and quercetin to commonly used cell culture media, Biochem. Biophys. Res. Commun. 273 (2000) 50–53.
[35] M. Akagawa, T. Shigemitsu, K. Suyama, Production of hydrogen peroxide by polyphenols and polyphenol-rich beverages under *quasi*-physiological conditions, Biosci. Biotechnol. Biochem. 67 (2003) 2632–2640.
[36] Y.L. Chen, J.Y. Wang, S.A. Chen, B.C. Yang, Granulocytes mediates the Fas-L-associate apoptosis during lung metastasis of melanoma that determines the metastatic behaviour, Br. J. Cancer 87 (2002) 359–365.